



HAL
open science

Accelerating the energy transition towards photovoltaic and wind in China

Yijing Wang, Rong Wang, Katsumasa Tanaka, Philippe Ciais, Josep Penuelas, Yves Balkanski, Jordi Sardans, Didier Hauglustaine, Wang Liu, Xiaofan Xing, et al.

► To cite this version:

Yijing Wang, Rong Wang, Katsumasa Tanaka, Philippe Ciais, Josep Penuelas, et al.. Accelerating the energy transition towards photovoltaic and wind in China. *Nature*, 2023, 619 (7971), pp.761 - 767. 10.1038/s41586-023-06180-8 . hal-04179048

HAL Id: hal-04179048

<https://hal.science/hal-04179048>

Submitted on 9 Aug 2023

HAL is a multi-disciplinary open access archive for the deposit and dissemination of scientific research documents, whether they are published or not. The documents may come from teaching and research institutions in France or abroad, or from public or private research centers.

L'archive ouverte pluridisciplinaire **HAL**, est destinée au dépôt et à la diffusion de documents scientifiques de niveau recherche, publiés ou non, émanant des établissements d'enseignement et de recherche français ou étrangers, des laboratoires publics ou privés.

Accelerating the energy transition towards photovoltaic and wind in China

<https://doi.org/10.1038/s41586-023-06180-8>

Received: 13 February 2022

Accepted: 9 May 2023

Published online: 26 July 2023

Open access

 Check for updates

Yijing Wang¹, Rong Wang^{1,2,3,4,5,6,7,8}, Katsumasa Tanaka^{8,9}, Philippe Ciais^{8,10}, Josep Penuelas^{11,12}, Yves Balkanski⁸, Jordi Sardans^{11,12}, Didier Hauglustaine⁸, Wang Liu¹, Xiaofan Xing¹, Jiarong Li¹, Siqing Xu¹, Yuankang Xiong¹, RuiPu Yang¹, Junji Cao¹³, Jianmin Chen^{1,2,3}, Lin Wang^{1,2,3}, Xu Tang^{2,3} & Renhe Zhang^{2,3}

China's goal to achieve carbon (C) neutrality by 2060 requires scaling up photovoltaic (PV) and wind power from 1 to 10–15 PWh year⁻¹ (refs. 1–5). Following the historical rates of renewable installation¹, a recent high-resolution energy-system model⁶ and forecasts based on China's 14th Five-year Energy Development (CFED)⁷, however, only indicate that the capacity will reach 5–9.5 PWh year⁻¹ by 2060. Here we show that, by individually optimizing the deployment of 3,844 new utility-scale PV and wind power plants coordinated with ultra-high-voltage (UHV) transmission and energy storage and accounting for power-load flexibility and learning dynamics, the capacity of PV and wind power can be increased from 9 PWh year⁻¹ (corresponding to the CFED path) to 15 PWh year⁻¹, accompanied by a reduction in the average abatement cost from US\$97 to US\$6 per tonne of carbon dioxide (tCO₂). To achieve this, annualized investment in PV and wind power should ramp up from US\$77 billion in 2020 (current level) to US\$127 billion in the 2020s and further to US\$426 billion year⁻¹ in the 2050s. The large-scale deployment of PV and wind power increases income for residents in the poorest regions as co-benefits. Our results highlight the importance of upgrading power systems by building energy storage, expanding transmission capacity and adjusting power load at the demand side to reduce the economic cost of deploying PV and wind power to achieve carbon neutrality in China.

Ambitions to achieve carbon neutrality are needed in all nations to limit global warming to below 2 °C in the Paris Agreement^{8,9}. Accelerating the penetration of renewables is a key pillar in climate mitigation¹⁰. Global decarbonization is not, however, progressing as fast as it should to meet the goals of the Paris Agreement^{11–13}. The world is probably on track for 2.8 °C of warming at the end of this century on the basis of current policies¹⁴. To achieve the global transition towards low-C economies, the 27th Conference of the Parties to the United Nations Framework Convention on Climate Change (COP27) recommended annual investments of US\$4–6 trillion (all currency values throughout the paper are in US dollars) to accelerate the penetration of renewables¹⁴. However, details on how these funds should be allocated among renewables remain unclear^{1,6}, requiring advanced spatially explicit models to optimize the existing power systems with geospatial details and coordinating infrastructure^{8,15}.

The rapid increase in global carbon dioxide (CO₂) emissions since 2000 has been driven mainly by the growing energy demand in developing countries⁸. Decarbonization may be more challenging in developing than developed countries¹⁶, but mitigation in developing countries is

indispensable for meeting the climate goals^{8–10}. China, with 18% of the global population and 28% of the global CO₂ emissions, has recently strengthened its nationally determined contribution with carbon neutrality target by 2060 (ref. 2). Among renewables, PV and wind power have wider ranges of application than hydropower⁶, generate less detrimental effects on food and ecosystems than bioenergy¹⁷ and probably entail lower costs than carbon capture and storage (CCS)¹⁸. Achieving carbon neutrality requires scaling up PV and wind power from 1 to 10–15 PWh year⁻¹ during 2020–2060 in China^{1–5,19}. This capacity, however, would only reach 5 PWh year⁻¹ assuming the annual growth rate of 100 TWh year⁻¹ from 2010–2020 (ref. 1) or 9 PWh year⁻¹ using forecasts by the governmental plans of CFED⁷ or 9.5 PWh year⁻¹ based on a recent high-resolution energy-system model⁶. There is also a chance that the growth of PV and wind power in China slows down owing to decreasing governmental subsidies²⁰, a lack of transmission infrastructure⁶ and restrictions for protecting agricultural, industrial and urban lands²¹.

A spatially explicit method is needed for performing an optimization of energy systems by coordinating the generation of power with transmission and consumption of electricity in a country as vast as

¹Shanghai Key Laboratory of Atmospheric Particle Pollution and Prevention (LAP³), Department of Environmental Science and Engineering, Fudan University, Shanghai, China. ²IRDR International Center of Excellence on Risk Interconnectivity and Governance on Weather/Climate Extremes Impact and Public Health, Fudan University, Shanghai, China. ³Institute of Atmospheric Sciences, Fudan University, Shanghai, China. ⁴Shanghai Frontiers Science Center of Atmosphere-Ocean Interaction, Shanghai, China. ⁵MOE Laboratory for National Development and Intelligent Governance, Fudan University, Shanghai, China. ⁶Institute of Eco-Chongming (IEC), Shanghai, China. ⁷National Observations and Research Station for Wetland Ecosystems of the Yangtze Estuary, Fudan University, Shanghai, China. ⁸Laboratoire des Sciences du Climat et de l'Environnement (LSCE), CEA/CNRS/UVSQ, Université Paris-Saclay, Gif-sur-Yvette, France. ⁹Earth System Division, National Institute for Environmental Studies (NIES), Tsukuba, Japan. ¹⁰Climate and Atmosphere Research Center (CARE-C), The Cyprus Institute, Nicosia, Cyprus. ¹¹CSIC, Global Ecology Unit CREAF-CSIC-UAB, Bellaterra, Spain. ¹²CREAF, Cerdanyola del Vallès, Spain. ¹³Institute of Atmospheric Physics, Chinese Academy of Sciences, Beijing, China. [✉]e-mail: rongwang@fudan.edu.cn

China²². Methods accounting for the spatial heterogeneity of PV and wind resources and demand for electricity transmission and storage have been developed for Europe²³ and the USA²⁴, but the flexibility of power load²⁵ and intertemporal dynamics of learning²⁶ have rarely been addressed in studies for China^{6,27–29}. In contrast to previous studies^{2,6,27–29}, we developed a unified optimization framework that accounts for the geospatial capacities of installing new PV panels and wind turbines, expansion of existing UHV transmission, storing energy, flexible power loads and dynamics of learning. Our research highlights the need for investments in upgrading power systems and infrastructure, as well as the co-benefits of increasing resident incomes.

Optimization of PV and wind power systems

We optimized the location, capacity and construction time of new PV and wind power plants each decade during 2021–2060 by minimizing the levelized cost of electricity (LCOE)^{6,27} (Extended Data Fig. 1). The LCOE is defined as the normalized present value of costs including initial investment, operation and maintenance (O&M), land acquisition, UHV transmission and energy storage that are divided by the power generated over the lifetime (25 years (ref. 30)) of power plants (see Methods). We optimized the number of pixels receiving new PV panels or wind turbines to minimize the LCOE (Extended Data Fig. 2). We identified respectively 2,767, 1,066 and 11 power plants of PV, onshore wind and offshore wind at the utility scale (>10 MW) by considering resource limitations, administrative boundaries, land suitability, restriction of land use, ground slope, land cover, latitude, longitude, terrestrial and marine ecological conservation, water depth at offshore wind stations, shipping routes, solar irradiance, wind power density and air temperature (Fig. 1a,b). The predicted location and capacity of power plants match the observed PV and wind power plants to some extent³¹ (Extended Data Fig. 3).

We identified diurnal variabilities and seasonal patterns of PV and wind power generation, which are not in phase with the profile of power demand (Fig. 1c). The power generation peaks in spring owing to variations in surface air temperature, shade, solar angle and inclination of PV panels (Extended Data Fig. 4). Our model considers the flexibility of power load whereby end users adjust hourly power demand to match the supply except for heating and cooling of houses and electric cars²⁵ (that is, 12% in total power demand by 2060) (see Methods). The adjusted power demand shifts in the daytime to match the peak of PV and wind power generation (Fig. 1c). Expanding the capacity of transmission by 6.4 TW and building new energy storage of 1.3 TW in China improves the efficiency of power use (Fig. 1d), whereas adopting a lower rate of electrification or considering a higher capacity of other types of renewable reduces the efficiency (Extended Data Fig. 5).

Similar to a previous study³², we estimated that the rate of learning in China during 2000–2020 could be higher than the rate measured in other regions during 1975–2020 (Supplementary Table 1). On this basis, optimizing the construction time of power plants reduces the LCOE of PV and wind power plants from \$0.067 to \$0.046 per kWh (Fig. 1e). This requires an increase in PV and wind investment from \$127 billion year⁻¹ in the 2020s to \$426 billion year⁻¹ in the 2050s. This investment profile is similar to CFED^{1,7} for the 2020s and 2030s but is lower in the 2040s and 2050s. Investment in our optimal path over the period 2031–2050 (\$220 billion year⁻¹) is lower than a previous estimate⁶ (\$320 billion year⁻¹) made without simulating the dynamics of learning.

We quantified the effects of optimization relative to a baseline scenario, which limits the capacity of PV and wind power plants to 10 GW without electricity transmission and energy storage and assumes that the growth rate of PV and wind power is constant during 2021–2060 without optimizing the dynamics of learning²⁶. We designed five

sensitivity experiments by sequentially increasing the limit of capacity for individual plants from 10 to 100 GW (case A), considering the construction of new UHV lines (case B), adding energy storage (case C), improving electrification of non-power sectors³³ from 0 to 58% (case D) and considering flexible power loads (case E). Case E becomes equivalent to our optimal path if the construction time of power plants is optimized through accounting for the dynamics of learning²⁶. Our optimal path increases the capacity the most by storing energy (+6.4 PWh year⁻¹ as a difference between cases B and C), but it reduces the costs the most by optimizing the dynamics of learning (–\$115 billion year⁻¹ as a difference between case E and the optimal path) (Fig. 1f).

Costs of CO₂ emissions reduction

We estimated the marginal abatement cost (MAC) at the plant level, which varies from –\$166 per tCO₂ to \$106 per tCO₂ in 2060 in our optimal path (Fig. 2a). For example, 77% of PV and wind power could be competitive against nuclear power with a lower MAC¹. The average abatement cost (–\$4.5 per tCO₂) for 9.5 PWh of power generation is lower than a previous estimate (\$27 per tCO₂) under an 80% renewable penetration in China⁶. The MAC increases as the capacity rises owing to techno-economic limits and differences in the prices of the substituted fossil fuel (Extended Data Fig. 6). Such behaviour of the MAC indicates an increase in the costs to install higher capacities of PV and wind power³⁴, even by considering the benefits of technological improvements²⁶.

The capacity of PV and wind power reaches 15 PWh in 2060 (9 PWh in the CFED plan⁷) with an average abatement cost of \$6 per tCO₂ (\$97 per tCO₂ in the CFED plan¹) (Fig. 2b,c). The CO₂ emissions were most abated by storing energy (+3.5 Gt CO₂) for power plants with MAC < \$100 per tCO₂ and by optimizing the dynamics of learning (+3.5 Gt CO₂) for power plants with MAC < \$0 per tCO₂. The costs of PV and wind power would increase if we assumed international learning rates (Supplementary Table 1), high capital costs³⁵, a short lifetime of power plants (20 years)³⁰ or a high discounting rate (7%)⁶, but decrease if we neglected the costs of new UHV lines or adopted low capital costs³⁶. For example, the average abatement cost increased from –\$2 to \$14 per tCO₂ if we increased the discounting rate from 3% to 7% to reduce the revenue from power generation, but it decreased from \$22 to \$0 per tCO₂ if we increased the lifetime of power plants from 15 to 35 years (Supplementary Fig. 1). The cost composition shifted from transformers and O&M to modules and land acquisition as we moved from the baseline case to the optimal path (Fig. 2d). A recent study showed that globalized supply chain reduces global solar-module prices³². Our results indicate that the impact of technological transformation between countries might be moderate for China with a fast decline in module prices (Supplementary Fig. 2).

Trade-offs among land, costs and power

We analysed the trade-offs among land requirements, costs and power capacity (Table 1). The capacity of PV and wind power could provide up to 59% of the projected total power demand in China for 2060, compared with a contribution of 20% by hydrogen, nuclear and biomass in a scenario keeping global warming below 1.5 °C by ref. 2. Expansion of PV and wind power from 1 to 15 PWh year⁻¹ requires 585,000 km² of land for placing PV panels and 672,000 km² of area for installing onshore and offshore wind turbines, in which 33%, 35%, 16% and 6% of facilities are distributed in deserts, grassland, oceans and cropland, respectively (Extended Data Table 1). Building these PV and wind power plants requires initial investment of \$201 billion year⁻¹ with O&M costs of \$47 billion year⁻¹, the sum of which is 7% of the total spending of China's public finances³⁷ in 2020. These costs can partly offset the income by saving costs of purchasing fossil fuels (\$223 billion year⁻¹) and reducing carbon costs (\$399 billion year⁻¹) by assuming a representative carbon price of \$100 per tCO₂ from the 1.5 °C scenario by ref. 2.

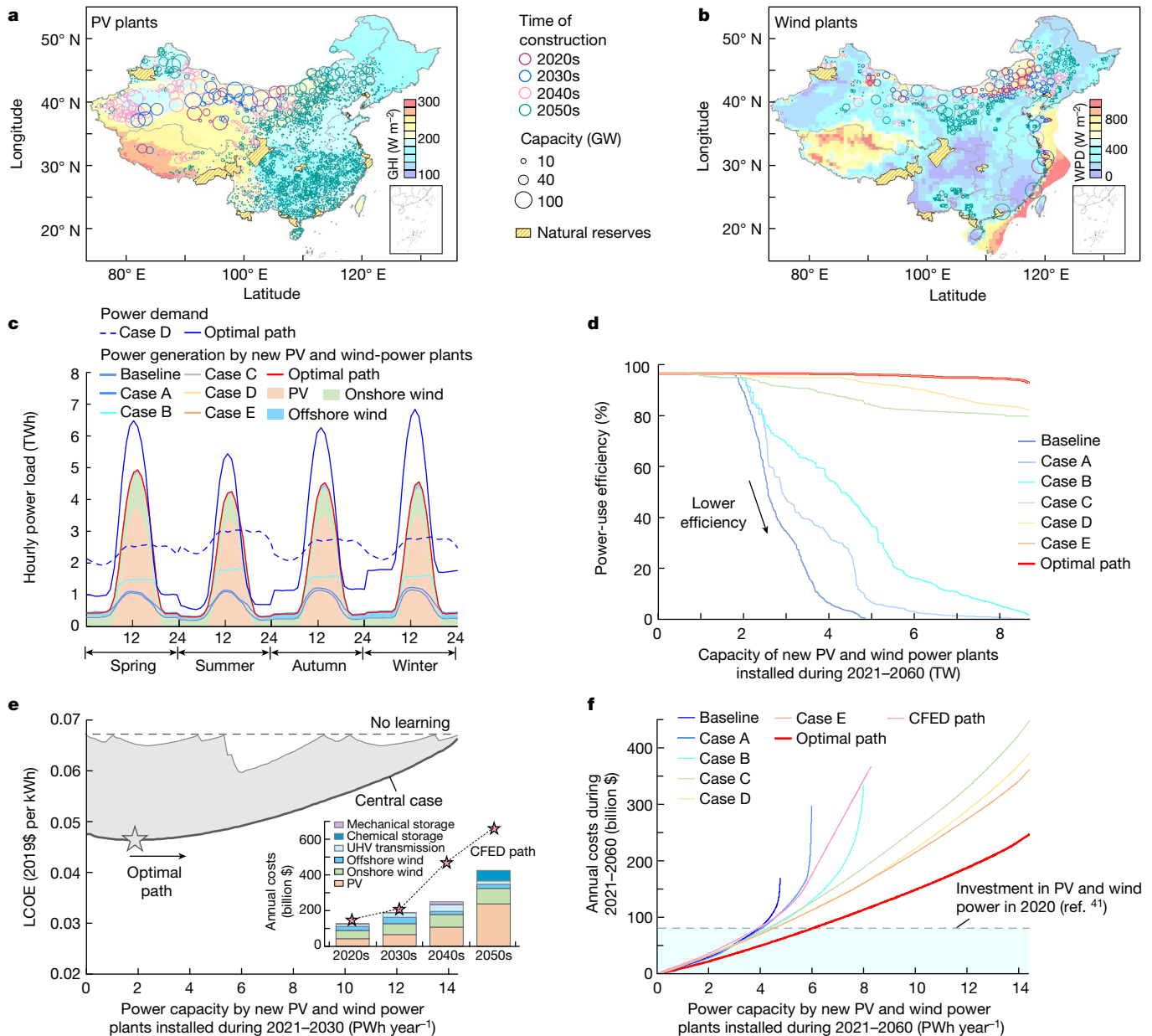


Fig. 1 | Optimization of the location, capacity and construction time of utility-scale PV and wind power plants during 2021–2060 in China. **a, b**, Maps of PV (**a**) and wind (**b**) power plants built by decade in the optimal path. The background shows global horizontal irradiance (GHI) and wind power density (WPD). **c**, Seasonal and diurnal variations in the generation and demand of power under an electrification rate of 58% for non-power sectors in 2060. The shading represents the PV and wind power generation without considering curtailments. In a baseline scenario, the capacity of individual PV and wind power plants is limited to 10 GW without electricity transmission and energy storage, whereas the growth rate of PV and wind power is constant during 2021–2060 without considering the dynamics of learning. We design five experiments by sequentially increasing the limit of power capacity from 10 to 100 GW (case A), building new UHV lines (case B), storing energy (case C), improving the electrification of non-power sectors (case D) and considering

flexibility of power loads (case E). Case E becomes equivalent to our optimal path if the construction time of power plants is optimized by accounting for the dynamics of learning. **d**, Power-use efficiency defined as the fraction of the generated power consumed by end users. **e**, Influences of increasing the capacity of new PV and wind power plants built in the 2020s on the LCOE of all new PV and wind power plants built during 2021–2060. The optimal path minimizes the LCOE by optimizing the construction time of individual power plants (shaded area) under a discounting rate of 5%. The inset shows the annual costs by decade. We consider a 'CFED path' by following the rate of installing renewables in China's 14th Five-year Energy Development (CFED)⁷ with the projected costs of PV and wind power¹. **f**, Dependency of the annual average costs of deploying PV and wind power during 2021–2060 on the power capacity of new PV and wind power plants built during 2021–2060 under different scenarios.

We predicted that 183 of 3,844 plants will be built with capacity >10 GW. The average abatement cost will decrease from \$62 to \$6 per tCO_2 as the limit of capacity for individual plants increases from 0.1 to 10 GW (Extended Data Fig. 7). The feasibility of building large power plants in China could be supported by commissions of the Jiuquan

onshore wind power plant at 20 GW and the Yanchi PV power plant at 1 GW, but it entails high requirements on grid integration, electricity transmission and initial investment³⁸. Non-economic factors such as ecological preservation, engineering feasibility and political impediment deserve attention.

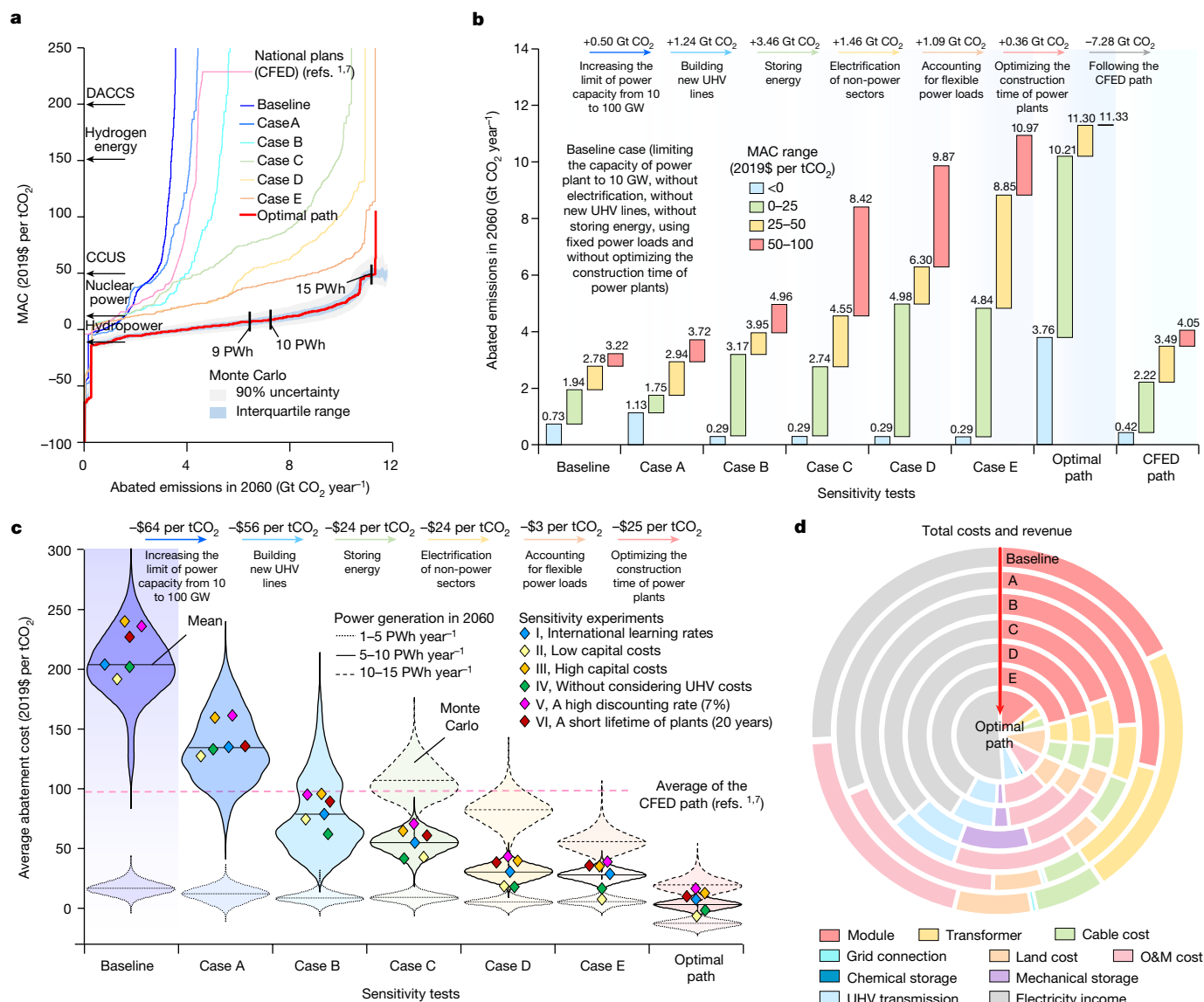


Fig. 2 | Costs of CO₂ emissions abatement in 2060 by deploying PV and wind power in China. **a**, The MAC under a 5% discounting rate in 2060. The configurations of the baseline case, cases A–E, the CFED case and our optimal path are identical to those defined in Fig. 1. Arrows represent the MACs for hydropower, nuclear power, hydrogen energy, carbon capture utilization and storage (CCUS) and direct air carbon capture and storage (DACCS)¹. **b**, Impacts of our optimizing procedures on the potential of CO₂ emissions reduction based on the ranges of MAC. **c**, Violin plots of the average abatement costs

when building new PV and wind power plants to meet the power demand in 2060. We perform sensitivity experiments by applying international learning rates (Supplementary Table 1) (I), adopting low³⁶ (II) or high³⁵ (III) capital costs, neglecting the costs of building new UHV lines (IV), adopting a high discounting rate (7%)⁶ (V) and assuming a short lifetime (20 years) of power plants³⁰ (VI). **d**, Composition of the costs and income when increasing PV and wind power generation from 1 to 10 PWh year⁻¹ to replace fossil fuel in 2060.

Implication for carbon neutrality

Many scenarios meeting the target of carbon neutrality⁸ rely on retrofitting existing plants with CCS, which may be limited by economic costs¹, geological constraints³⁹ and biomass availability¹⁷. We analysed the impact of deploying PV and wind power on the demand for CCS with fossil fuel² or bioenergy¹⁷ to achieve carbon neutrality in 2060 by considering terrestrial carbon sinks, electrification of non-power sectors (58%)³³ and power supply by other renewables² (Fig. 3). A transition from CFED⁷ to our optimal path reduces the demand for CCS from 8.9 to 2.8 PWh year⁻¹ in 2060 (Fig. 3a). The share of PV and wind in power supply increases from 12% to 59% during 2021–2060 at an annual rate of 1.8%, 1.4%, 1.0% and 0.7% in the 2020s, 2030s, 2040s and 2050s, respectively, which requires acceleration relative to an annual rate of 1% for China in the 2010s⁴⁰. Although the projected annual growth rates

for wind (1%) and PV (0.8%) in China during the 2020s are comparable with the maximal annual rates of 1% in Spain, 0.9% in Turkey and 0.6% in the USA and New Zealand for wind or 1.1% in Japan and 1% in Germany for PV¹³, the expansion of these technologies may present greater challenges in China because of her larger absolute power demand⁴.

Upgrading power systems is crucial to accelerating the penetration of renewables in China^{7,27–29}. For example, the growth of PV and wind power does not depend on investment in electricity transmission in CFED plans⁷ (Fig. 3c). By contrast, our model optimizes the dynamics of learning (Extended Data Fig. 8) and the strategy of energy storage (Extended Data Fig. 9) by accounting for investment in UHV lines (Fig. 3b). An example of the findings shows that, with the increase in PV and wind investment from \$0 to \$60 billion year⁻¹ over the period 2021–2060, the ratio of cost reduction for PV, wind and CCS to the increase in costs for PV and wind power is 2.7:1 in the optimal path towards carbon

Table 1 | Capacity, land acquisition and annual costs of new PV and wind power plants built during 2021–2060 under a discounting rate of 5%

Annual power generation by PV and wind power plants (PWh year ⁻¹)	Total area (Mha)	Length of new UHV lines (million km)	Capacity of energy storage (TW)	Number of new PV and wind power plants	Number of new PV and wind power plants with capacity >10GW	Average power capacity (GW)	Average capacity factor (%)	Annual cost of electricity transmission (billion \$ year ⁻¹)	Annual cost of energy storage (billion \$ year ⁻¹)	Annual initial investment cost (billion \$ year ⁻¹)	Annual O&M cost (billion \$ year ⁻¹)	Average abatement costs (\$ per tCO ₂)
1–5	29.05	0.46	0	153	48	14.33	20.59	10.49	0	47.68	10.50	-3.70
5–10	47.93	0.46	0.42	619	77	4.60	19.97	8.58	6.43	62.86	16.95	0.61
10–15	43.02	0.21	0.88	3,023	55	1.10	17.00	3.83	12.74	82.97	16.07	15.69
Total	132.05	1.14	1.34	3,844	183	2.26	18.84	23.35	19.87	201.21	46.58	5.73

neutrality in 2060, which is lower than the ratio of 6.4:1 in CFED plans⁷. This ratio increases to 5.4:1 in our optimal path when investment in PV and wind power systems increases from \$60 to \$250 billion year⁻¹, but decreases to 0.4:1 in CFED plans⁷. Our results highlight the importance of ramping up PV and wind investment relative to current levels (\$77 billion year⁻¹ in 2020)⁴¹ to reduce the economic costs of achieving carbon neutrality.

Implication for alleviating poverty

Deploying renewables has been suggested as an effective way to reduce poverty⁴² by generating revenue from wealthier regions. This impact, however, has not been assessed by a national cost–benefit analysis in China. A higher carbon price generates more revenue for PV and wind power by saving more carbon costs (Fig. 4a). Accounting for the finances embodied in the transmission of electricity (see Methods), we found that the revenue from PV and wind power could be redistributed from the more developed east to the less developed west. Distributing the revenue to less-developed regions as the carbon price increases from \$0 to \$100 per tCO₂ removes 21 million people from the low-income group (<\$5,000 year⁻¹) and adds 6 million people to the high-income group (>\$20,000 year⁻¹) (Fig. 4b,c).

Increasing the carbon price from \$0 to \$100 per tCO₂ reduces income equality, with a decrease in the Gini coefficient from 0.453 to 0.441 (Fig. 4d). Adopting a carbon price of \$100 per tCO₂ generates a financial flow of \$1,055 billion in the transmission of PV and wind power in 2060, which is 15-fold higher than China’s annual investment in poverty alleviation during 2014–2020 (ref. 37). The generation of PV and wind power is dominated by Northwest China (5.9 PWh year⁻¹) and North China (5.2 PWh year⁻¹), whereas the consumption is dominated by East China (5.7 PWh year⁻¹) and Central China (4.3 PWh year⁻¹). The transmission of electricity leads to the largest finance flow (\$223 billion year⁻¹) from East China to Northwest China (Fig. 4e). By increasing the carbon price from \$0 to \$100 per tCO₂, deployment of PV and wind power benefits the poorest residents, with an increase in per-capita income from \$29,000 to \$34,400 in North China and from \$29,100 to \$30,600 in Northwest China.

Implication for climate policies

The gap between current decarbonization rates and the levels required to achieve carbon neutrality remains substantial^{8–10}. China has been at the forefront of PV deployment since 2009 (ref. 27), accompanied by an accelerated growth of wind power¹. Despite these accomplishments,

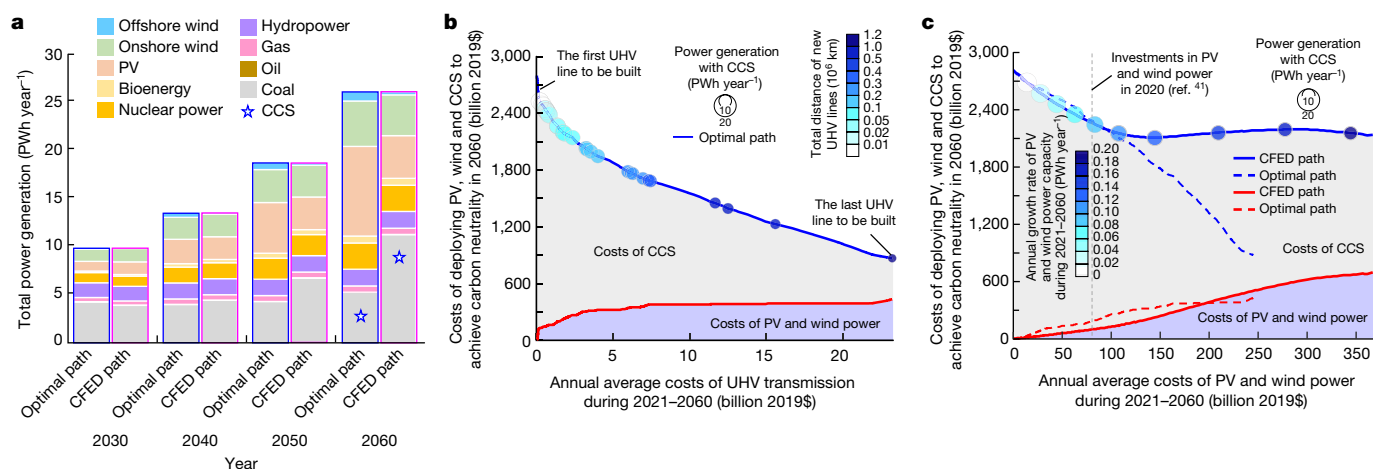


Fig. 3 | Different paths to achieve carbon neutrality in China by 2060.

a, Composition of the generated power by decade. The projected generation of power by oil, gas, bioenergy, nuclear power and hydropower are derived from the ‘1.5-°C-limiting’ scenario in a multi-model study². The PV and wind power are projected by our optimal path and CFED⁷. Assuming that coal meets the remaining power demand, we estimate the demand for CCS installed with fossil fuel or biomass when achieving carbon neutrality in 2060. **b**, Dependence of the annual costs of PV, wind and CCS when achieving carbon neutrality by 2060 on the costs of transmitting electricity by UHV lines during 2021–2060 in the optimal path. **c**, Dependence of the annual costs of PV, wind and CCS when

achieving carbon neutrality by 2060 on the costs of PV and wind power during 2021–2060 in our optimal (dashed lines) path and CFED⁷ (solid lines). **In b**, the total capacity of PV and wind power plants built during 2021–2060 in the optimal path depends on the capacity of electricity transmission, whereas the total distance of new UHV lines is indicated by the colour of the circle. The total capacity of PV and wind power built by 2060 in CFED⁷ depends on the annual growth rate of PV and wind power during 2021–2060, which is indicated by the colour of the circles in **c**. We predict the costs of CCS based on the MAC of CCS¹ and the demand for CCS when achieving carbon neutrality by 2060 under different scenarios.

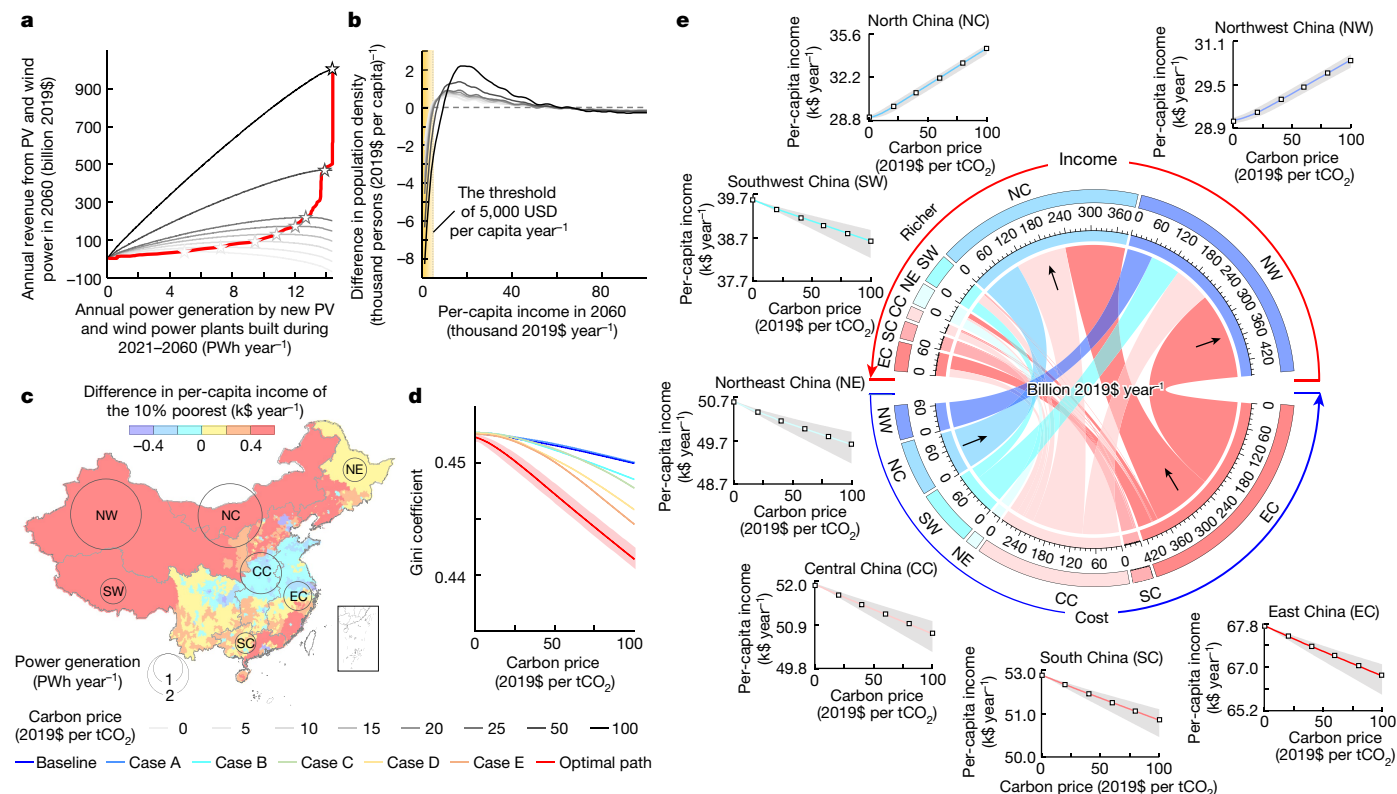


Fig. 4 | Co-benefits of deploying PV and wind power on poverty alleviation in China. **a**, Revenue from PV and wind power generation in 2060 under different carbon prices. **b**, Change in the distribution of per-capita income when the carbon price increases from \$0 to \$100 per tCO₂. **c**, Change in the income of the 10% poorest people in 2060 owing to the deployment of PV and wind power during 2021–2060 under the carbon price of \$100 per tCO₂. **d**, Variation in the

Gini coefficient when the carbon price increases from \$0 to \$100 per tCO₂. The shaded area represents the 90% uncertainty in Monte Carlo simulations. **e**, Flow of finances embodied in the transmission of electricity generated by new PV and wind power plants built during 2021–2060 under the carbon price of \$100 per tCO₂. The insets show the variations in per-capita income by region when the carbon price increases from \$0 to \$100 per tCO₂ in 2060.

it remains challenging to achieve carbon neutrality by 2060. As fossil fuels continue to dominate energy-related investments¹², renewable growth could slow down as subsidies for companies generating PV and wind power decline^{20,21}. Unlike previous studies^{1,2,6,27–29}, our research reveals greater potential for PV and wind power generation in China, alongside the need for larger investment in power-system upgrades.

Our approach enhances the optimization of PV and wind power systems^{2,6,27–29} by applying a spatially explicit method that provides insights into climate mitigation in countries beyond China¹⁴. First, deeper decarbonization requires greater investments in renewables because of physical constraints in abating more CO₂ emissions (for example, larger demand for land and infrastructure), even when accounting for technological improvements^{26,30}. Despite the projection of decreasing renewable energy costs⁴³, we emphasize the importance of policy interventions (for example, building large PV and wind power plants, grid integration, energy storage and demand-side power-load management) to reduce renewable costs. Second, deploying PV and wind power can offer new sources of income in less-developed regions with vast areas of desert and marginal lands. It has implication for accelerating economic development by deploying renewables in semiarid regions such as Africa and the Middle East⁴⁴. Third, optimizing power systems for large developing countries can lower the costs of deploying renewables in the upcoming decades, making it feasible to achieve more ambitious climate targets beyond the 2060 carbon neutrality⁴⁵. Our research highlights the technical and physical constraints on deploying renewables to mitigate CO₂ emissions, the importance of scaling up investments to accelerate energy transition to PV and wind power and the optimal route to achieve carbon neutrality in the long run.

Online content

Any methods, additional references, Nature Portfolio reporting summaries, source data, extended data, supplementary information, acknowledgements, peer review information; details of author contributions and competing interests; and statements of data and code availability are available at <https://doi.org/10.1038/s41586-023-06180-8>.

1. Carbonomics. *China Net Zero: The Clean Tech Revolution* (Goldman Sachs Research, 2021); <https://www.qa.goldmansachs.com/insights/pages/gs-research/carbonomics-china-netzero/report.pdf>.
2. Duan, H. et al. Assessing China's efforts to pursue the 1.5°C warming limit. *Science* **372**, 378–385 (2021).
3. Liu, L. et al. Potential contributions of wind and solar power to China's carbon neutrality. *Resour. Conserv. Recycl.* **180**, 106155 (2022).
4. Zhang, S. & Chen, W. Assessing the energy transition in China towards carbon neutrality with a probabilistic framework. *Nat. Commun.* **13**, 87 (2022).
5. Zhuo, Z. et al. Cost increase in the electricity supply to achieve carbon neutrality in China. *Nat. Commun.* **13**, 3172 (2022).
6. Chen, X. et al. Pathway toward carbon-neutral electrical systems in China by mid-century with negative CO₂ abatement costs informed by high-resolution modeling. *Joule* **5**, 2715–2741 (2021).
7. *Research on China's Energy Transition and 14th Five-year Power Planning* (Global Energy Interconnection Development and Cooperation Organization, 2020); <http://www.chinasmartgrid.com.cn/news/20200803/636327.shtml>.
8. IPCC. The numbers behind the science. In *Climate Change 2014: Mitigation of Climate Change* (Cambridge Univ. Press, 2022); <https://www.ipcc.ch/assessment-report/ar6/>.
9. Meinshausen, M. et al. Realization of Paris Agreement pledges may limit warming just below 2 °C. *Nature* **604**, 304–309 (2022).
10. Tanaka, K. et al. Paris Agreement requires substantial, broad, and sustained policy efforts beyond COVID-19 public stimulus packages. *Clim. Change* **172**, 1 (2022).
11. *Emissions Gap Report 2022* (UNEP, 2022); <https://www.unep.org/resources/emissions-gap-report-2022>.
12. Organisation for Economic Co-operation and Development (OECD). Support for fossil fuels almost doubled in 2021, slowing progress toward international climate goals,

- according to new analysis from OECD and IEA <https://www.oecd.org/newsroom/support-for-fossil-fuels-almost-doubled-in-2021-slowing-progress-toward-international-climate-goals-according-to-new-analysis-from-oecd-and-iea.htm> (2022).
13. Cherp, A., Vinichenko, V., Tosun, J., Gordon, J. & Jewell, J. National growth dynamics of wind and solar power compared to the growth required for global climate targets. *Nat. Energy* **6**, 742–754 (2021).
 14. *World Energy Outlook 2022* (IEA, 2022); <https://www.iea.org/reports/world-energy-outlook-2022>.
 15. Klaaßen, L. & Steffen, B. Meta-analysis on necessary investment shifts to reach net zero pathways in Europe. *Nat. Clim. Change* **13**, 58–66 (2023).
 16. Heuberger, C. F. & Dowell, N. M. Real-world challenges with a rapid transition to 100% renewable power systems. *Joule* **2**, 367–370 (2018).
 17. Xu, S. et al. Delayed use of bioenergy crops might threaten climate mitigation and food security. *Nature* **609**, 299–306 (2022).
 18. Grant, N. et al. Cost reductions in renewables can substantially erode the value of carbon capture and storage in mitigation pathways. *One Earth* **4**, 1588–1601 (2021).
 19. Xia, N. Four research teams powering China's net-zero energy goal. *Nature* **603**, S41–S43 (2022).
 20. Li, J. & Huang, J. The expansion of China's solar energy: challenges and policy options. *Renew. Sustain. Energy Rev.* **132**, 110002 (2020).
 21. Standaert, M. Why China's renewable energy transition is losing momentum. *Yale Environment 360* <https://e360.yale.edu/features/why-chinas-renewable-energy-transition-is-losing-momentum> (2019).
 22. Xing, X. et al. Spatially explicit analysis identifies significant potential for bioenergy with carbon capture and storage in China. *Nat. Commun.* **12**, 3159 (2021).
 23. Schlachterberger, D. P., Brown, T., Schramm, S. & Greiner, M. The benefits of cooperation in a highly renewable European electricity network. *Energy* **134**, 469–481 (2017).
 24. Jacobson, M. Z. et al. Low-cost solution to the grid reliability problem with 100% penetration of intermittent wind, water, and solar for all purposes. *Proc. Natl Acad. Sci. USA* **112**, 15060–15065 (2015).
 25. Brown, T. & Reichenberg, L. Decreasing market value of variable renewables can be avoided by policy action. *Energy Econ.* **100**, 105354 (2021).
 26. Victoria, M., Zhu, K., Brown, T., Andresen, G. B. & Greiner, M. Early decarbonisation of the European energy system pays off. *Nat. Commun.* **11**, 6223 (2020).
 27. Lu, X. et al. Combined solar power and storage as cost-competitive and grid-compatible supply for China's future carbon-neutral electricity system. *Proc. Natl Acad. Sci. USA* **118**, e2103471118 (2021).
 28. Li, M. et al. High-resolution data shows China's wind and solar energy resources are enough to support a 2050 decarbonized electricity system. *Appl. Energy* **306**, 117996 (2022).
 29. He, G. & Kammen, D. M. Where, when and how much solar is available? A provincial-scale solar resource assessment for China. *Renew. Energy* **85**, 74–82 (2016).
 30. Victoria, M. et al. Solar photovoltaics is ready to power a sustainable future. *Joule* **6**, 1041–1056 (2021).
 31. Dunnett, S. et al. Harmonised global datasets of wind and solar farm locations and power. *Sci. Data* **7**, 130 (2020).
 32. Helveston, J. P., He, G. & Davidson, M. R. Quantifying the cost savings of global solar photovoltaic supply chains. *Nature* **612**, 83–87 (2022).
 33. *An Energy Sector Roadmap to Carbon Neutrality in China* (IEA, 2021); <https://www.iea.org/reports/an-energy-sector-roadmap-to-carbon-neutrality-in-china>.
 34. Kramer, G. J. & Haigh, M. No quick switch to low-carbon energy. *Nature* **462**, 568–569 (2009).
 35. Lorenczik, S. et al. Projected costs of generating electricity—2020 edition. *International Energy Agency, Nuclear Energy Agency, Organisation for Economic Co-Operation and Development* <https://www.iea.org/reports/projected-costs-of-generating-electricity-2020> (2020).
 36. China Electricity Council. Main indicators of national economy in 2020 <https://www.cec.org.cn/upload/1/editor/1640595481946.pdf> (2021).
 37. Central People's Government of the People's Republic of China. A press conference of the Ministry of Finance introduced fiscal revenue and expenditure in 2020 http://www.gov.cn/xinwen/2021-01/28/content_5583244.htm (2021).
 38. Rakhshani, E., Rouzbehi, K. J., Sánchez, A., Tobar, A. C. & Poursmaeil, E. Integration of large scale PV-based generation into power systems: a survey. *Energies* **12**, 1425 (2019).
 39. Lane, J., Greig, C. & Garnett, A. Uncertain storage prospects create a conundrum for carbon capture and storage ambitions. *Nat. Clim. Change* **11**, 925–936 (2021).
 40. U.S. Energy Information Administration. Annual energy review <https://www.eia.gov/totalenergy/data/annual/#summary> (2023).
 41. Insight & Info. China Solar Power Industry Development Status Research and Investment Prospects Forecast for 2022–2029. Insight and Info Consulting Ltd http://www.360doc.com/content/22/1024/13/13672581_1053082374.shtml (2022).
 42. Zhang, H. et al. Solar photovoltaic interventions have reduced rural poverty in China. *Nat. Commun.* **11**, 1969 (2020).
 43. Ives, M. et al. A new perspective on decarbonising the global energy system https://www.ucl.ac.uk/climate-action-unit/sites/climate_action_unit/files/energy_transition_spm_ch.pdf (2021).
 44. Creutzig, F. et al. The underestimated potential of solar energy to mitigate climate change. *Nat. Energy* **2**, 17140 (2017).
 45. Matthews, H. D. & Wynes, S. Current global efforts are insufficient to limit warming to 1.5°C. *Science* **376**, 1404–1409 (2022).

Publisher's note Springer Nature remains neutral with regard to jurisdictional claims in published maps and institutional affiliations.



Open Access This article is licensed under a Creative Commons Attribution 4.0 International License, which permits use, sharing, adaptation, distribution and reproduction in any medium or format, as long as you give appropriate credit to the original author(s) and the source, provide a link to the Creative Commons licence, and indicate if changes were made. The images or other third party material in this article are included in the article's Creative Commons licence, unless indicated otherwise in a credit line to the material. If material is not included in the article's Creative Commons licence and your intended use is not permitted by statutory regulation or exceeds the permitted use, you will need to obtain permission directly from the copyright holder. To view a copy of this licence, visit <http://creativecommons.org/licenses/by/4.0/>.

© The Author(s) 2023

Geospatial data in this study

An overview of our optimization model is shown in Extended Data Fig. 1. We optimized the placement and capacity of PV and wind power plants in our model driven by geospatial data (Supplementary Method 1), including land cover, solar radiation, wind speed, surface air temperature, ground slope, latitude and longitude of the installed PV panels, terrestrial and marine ecological reserves, water depths of offshore stations and marine shipping routes (Supplementary Table 2). All land pixels were categorized into forest, shrubland, savannah, grassland, wetland, cropland, urban and built-up land, mosaics of natural vegetation, snow and ice, deserts and water bodies⁴⁶. The suitability of the installation of PV panels or wind turbines was defined by land cover (Supplementary Table 3). Onshore wind turbines with the capacity of 2–2.5 MW and offshore wind turbines with the capacity of 5–10 MW are considered as the main models used in China at present⁴⁷, so we considered models for onshore (General Electric 2.5 MW) and offshore (Vestas 8.0 MW) wind power plants (Supplementary Table 4) at a hub height of 100 m above the ground to convert air kinetic energy to electricity based on the recommended power-generation curve⁴⁸ (Supplementary Fig. 3). Resources of solar and wind energy were associated with seasonal and diurnal variabilities and interannual differences. We estimated hourly solar radiation and wind speed at a hub height of 100 m above the ground as averages for 2012–2018 to provide a representative estimate of solar and wind energy in China (Supplementary Method 2). All geospatial data were projected to a resolution of 0.0083° in latitude and 0.033° in longitude for estimating the potential of power generation by installing PV panels or wind turbines in each pixel (Supplementary Methods 3–5).

The optimization model

We estimated the LCOE of the PV and wind power systems to indicate the grid parity of power generation, which is defined as the normalized net present value of all costs of investments, O&M, land acquisition, transmission and energy storage divided by the power generated during the lifetime (25 years (ref. 30)) of the PV and wind power plants³⁵. Before solving the optimization problem, we sought the best strategy for installing PV panels or wind turbines with different shapes to achieve the maximal capacity of power generation in each county (Supplementary Fig. 4). We took the number of pixels installing PV panels or wind turbines and the time to build each PV or wind power plant by decade as decision variables. By accounting for the intertemporal dynamics of learning^{26,30}, we developed a unique method to optimize the capacity of each power plant, the order of building power plants, the time to build each power plant and the option of energy storage when building a new power plant by solving a cost-minimization problem based on the LCOE for generating power by the projected PV and wind power plants:

$$\min_{\epsilon, n_x, t_x, s_x} \text{LCOE}_\epsilon = \frac{(V_\epsilon + A_\epsilon) \cdot \left[1 + R_y \cdot \sum_{t=1}^T \frac{1}{(1+r_d)^{tP}} \right] + G_\epsilon \cdot \sum_{t=1}^{L_g} \frac{1}{(1+r_d)^{tG}}}{E_\epsilon \cdot \sum_{t=1}^T \frac{1}{(1+r_d)^t}} \quad (1)$$

$$V_\epsilon = \sum_{q=1}^7 \sum_{x=1}^{n_q} [1 - \xi_x(t_x)] \cdot V_x(n_x), \quad x \in q \quad (2)$$

$$E_\epsilon = \sum_{h=1}^{8,760} \left[\sum_{q=1}^7 \sum_{x=1}^{n_q} E_{x,h}(n_x) - \eta_{tra} \Theta_h - \eta_{store} \Lambda_h \right], \quad x \in q \quad (3)$$

$$\Theta_h = \sum_{q=1}^7 \max \left[0, \sum_{x=1}^{n_q} E_{x,h}(n_x) - M_{q,h} \right] = \sum_{q=1}^7 U_{q,h}, \quad x \in q \quad (4)$$

$$\Lambda_h = \sum_{q=1}^7 \max \left[0, \sum_{x=1}^{n_q} E_{x,h}(n_x) + U_{q,h} - M_{q,h} \right], \quad x \in q \quad (5)$$

in which ϵ is a new power plant ($\epsilon = 1$ to 3,844), x is a power plant built before ϵ , n_x is the number of pixels installing PV panels or wind turbines in plant x , t_x is the time to build plant x , s_x is the option of energy storage (1 for pumped hydro and 2 for chemical batteries) when building plant x , T is the average lifetime of a power plant, h is hour, q is a region (1–7 for Central China, East China, North China, Northeast China, Northwest China, South China and Southwest China, respectively), n_q is the number of power plants in region q , r_d is the discounting rate (5%)², τ_p is a year in the operation of plant x , τ_g is a year during operation of energy storage in plant x , L_g is the lifetime of storage (50 years for pumped hydro⁶ and 15 years for chemical batteries⁴⁹), E_ϵ is the total power generation, V_ϵ is the total investment in power plants, A_ϵ is the total cost of electricity transmission, G_ϵ is the total cost of storage, R_y is the ratio of O&M costs to investment costs (1% for PV⁵⁰ and 3% for onshore and offshore wind power plants⁵¹), V_x is the investment in plant x , ξ_x is the ratio of cost reduction by learning when building plant x , $E_{x,h}$ is the hourly generation of power in a county, Θ_h is the hourly transmission of electricity, Λ_h is the hourly storage of electricity, η_{tra} is the fraction of electricity lost during transmission, η_{store} is the fraction of electricity lost during storage, $M_{q,h}$ is the hourly consumption of electricity in region q and $U_{q,h}$ is the hourly transmission of electricity from other regions to region q .

We optimized the increase in power capacity at an interval of 10 years during 2021–2060 because it generally takes 10 to 20 years for new technologies to be widely applied⁵². Given the variation of renewable energy within a decade, we performed a sensitivity experiment by optimizing the model at an interval of 5 years, in which the installed PV and wind power capacity and total costs both change moderately (Extended Data Fig. 8). Nevertheless, simulating the penetration of renewable energy within a decade will be useful to improve the optimization model.

We considered the connection of power plants in a county to one of the substations from the UHV transmission lines projected in the CFED plan⁷ (Supplementary Data Set 1) with the costs of building new UHV lines (Supplementary Method 6) and developing systems for storing energy (Supplementary Method 7). We estimated $U_{q,h}$ using three assumptions. First, the electricity generated by all PV and wind power plants in a region is used to meet the power demand in this region as a priority. Second, the extra electricity is connected to a substation in the UHV line and transmitted to a region in which the next substation in the line is located. Third, the electricity transmitted to a region is distributed to each county based on the distribution of the consumption of electricity in this region. We have considered the impact of transmission access on where and when to build new PV and wind power plants. When optimizing the construction time of 3,844 PV and wind power plants, we have accounted for the costs of building new UHV transmission lines when a new power plant is built, which influences the LCOE of this plant and the construction time of all new plants. By optimizing the construction time of each new power plant, we considered that a new UHV line required for this new plant will be constructed at the same time.

As a caveat of this study, we do not have explicit information for all UHV transmission lines, so we assumed that the UHV lines projected by the central government are used as a proxy for UHV lines between the main regions in the country. This assumption is useful to determine the demand for electricity transmission between regions, but it could lead to bias in our cost estimation because of the lack of detailed information for all UHV lines. For example, the projection of 128 UHV lines with a capacity of 12 GW each from Huaidong to Wan’an in our model indicates that at least a total transmission capacity of 1,536 GW is required for transmitting electricity from the region centred in Huaidong to the region centred in Wan’an, but the ultimate UHV lines built between

these two regions might be different from our prediction. This limitation can be addressed when the detailed information for all UHV transmission lines are available. To consider the outflow of electricity generated in a county, we sought the substation of UHV lines that is closest to this county and then we estimated the cost of electricity transmission from this county to the transmission substation and the cost of electricity transmission using one of the UHV lines. Although this study projected the construction of a large transmission capacity to optimize power systems, it is important to account for the physical, technical and economic constraints. These include the demand for advanced polymer matrix composites that can operate under a voltage of >1,000 kV, the construction of UHV lines over challenging terrains, the maintenance of these lines and ensuring the security of electricity transmission under extreme weather conditions.

We sought the optimal system for storing energy when building a new power plant using either mechanical storage (pumped hydro) with a lifetime of 50 years and a round-trip efficiency of 70% or chemical storage (batteries) with a lifetime of 15 years and a round-trip efficiency of 85% (see the parameterization of two systems in Supplementary Table 5) to minimize the LCOE (Extended Data Fig. 9).

Last, ξ_x is calculated as a function of the total capacity of installed PV or wind power (Supplementary Method 8) based on the measured rates of learning in China (Supplementary Table 1). We examined the sensitivity to adopting the international rates of learning in our model (Fig. 2c).

Capacity and costs of power generation

For a new PV or wind power plant x , the annual generation of power was calculated:

$$E_{x,h} = \sum_{j=1}^{8,760} \sum_{i=1}^{n_x} W_{i,j} \quad (6)$$

in which i is a pixel, j is the number of hours in a year and $W_{i,j}$ is the hourly generation of power in a pixel installing PV panels (calculated in Supplementary Method 3), onshore wind turbines (calculated in Supplementary Method 4) or offshore wind turbines (calculated in Supplementary Method 5). The parameters used to estimate the projected PV and wind power generation are listed in Supplementary Table 6.

The investment cost of a new PV or onshore wind power plant x was calculated⁶:

$$V_x = \sum_{i=1}^{n_x} (\mu_{\text{fix}} P_i + \mu_{\text{land}} S_i) + 2\mu_{\text{line}} \sqrt{\pi \sum_{i=1}^{n_x} S_i} + \mu_{\text{tran}} \text{int} \left(\frac{\sum_{i=1}^{n_x} P_i}{P_{\text{fix}}} \right) \quad (7)$$

in which i is a pixel, P_i is the installed capacity of PV panels (calculated in Supplementary Method 3) or onshore wind turbines (calculated in Supplementary Method 4), S_i is the area of pixels installing PV panels or wind turbines, P_{fix} is the capacity of a voltage transformer (300 MW), μ_{fix} is unit capital costs, μ_{land} is unit cost of land acquisition, μ_{line} is unit cost of line connection and μ_{tran} is unit cost of voltage transformation.

We assumed that the installed voltage transformer has a capacity of 300 MW (ref. 53). When estimating the unit cost of land acquisition, we considered that onshore wind turbines take up only 2% of area in a pixel and PV panels take up 100% of area in a pixel⁵⁴. We derived μ_{fix} as the sum of costs for modules (μ_{module}), inverters (μ_{inverter}), mounting materials (μ_{mounting}), secondary equipment (μ_{sec}), installation (μ_{ins}), administration (μ_{adm}) and grid connection (μ_{grid}) using the data for PV panels (\$0.64 per watt) published by the China Photovoltaic Industry Alliance⁵⁵ and using the data for onshore wind turbines (\$0.68 per watt) from a previous study⁵⁶. We demonstrated the impact of using different capital costs by examining the sensitivity to adopting high capital costs (\$0.73 and \$0.88 per watt for PV panels and onshore wind turbines, respectively)³⁵ or low capital costs (\$0.23 and \$0.76 per watt for PV panels and onshore wind turbines, respectively)³⁶ in the sensitivity tests (Fig. 2c).

The investment cost of an offshore wind power plant x was calculated on the basis of the distance of offshore wind turbines in this power plant to the onshore power station⁵⁷:

$$V_x = \sum_{i=1}^{n_x} [\mu_{\text{baseline}} (z_0 + z_1 D_{L,i}) (z_2 + z_3 D_{P,i}) P_i] \quad (8)$$

in which i is a pixel, μ_{baseline} is the unit cost of offshore wind turbines, P_i is the installed capacity of offshore wind turbines (calculated in Supplementary Method 5), $D_{L,i}$ is the distance of the offshore wind turbines to the onshore power station and $D_{P,i}$ is the water depth of the installed offshore wind turbines. The coefficients z_0 (0.0057), z_1 (0.7714), z_2 (0.0084) and z_3 (0.8368) were calibrated using engineering data⁵⁷. The parameters used to determine the costs of PV and wind power generation are listed in Supplementary Table 7. The parameters used to determine the costs of UHV transmission and energy storage are listed in Supplementary Table 8.

We adopted a fixed ratio of O&M costs to investment costs for the projected PV and wind power plants^{50,51}. We adopted 25 years (ref. 30) as the average lifetime of PV or wind power plants. We considered the costs of electricity transmission by UHV when increasing the installed capacity of a power plant. We sought the geographic centre among all pixels suitable for power generation and then increased the number of surrounding pixels (n_x) installing PV panels or wind turbines. The capacity of power generation by each power plant increases as the number of pixels installing PV panels or wind turbines increases in the order of the distance to the geographic centre. The inclusion of more pixels in a power plant, however, increases not only the capacity of this PV or wind power plant but also the total costs in the power systems. The LCOE for a new power plant first decreased when we increased the power capacity by increasing the number of pixels for installation of PV panels or wind turbines, because the capital costs were divided by the generated power, but then increased owing to the increasing costs of purchasing land and the decreasing power-use efficiency (Extended Data Fig. 2). We sought the optimal capacity for each power plant for achieving the minimum of the LCOE.

MAC

We assumed that the electricity generated by new PV and wind power plants was used to replace oil, gas and coal in the order of fuel price to produce the highest profits⁶. Solving the cost-minimization problem in equation (1) was constrained by the target of the annual abatement of CO₂ emissions by substituting fossil fuels when a new PV or wind power plant ϵ was built (F_ϵ):

$$F_\epsilon = \theta_{\text{fossil}} \cdot E_\epsilon - \sum_{q=1}^7 \sum_{x=1}^{n_q} (\gamma_x \cdot S_x) - \frac{\sum_{q=1}^7 \sum_{x=1}^{n_q} (\nu_x \cdot S_x)}{25}, \quad x \in q \quad (9)$$

in which E_ϵ is the total power generation, S_x is the area of pixels installing PV panels or wind turbines, θ_{fossil} is the CO₂ emission factor of coal (0.84 kg CO₂ kWh⁻¹), oil (0.72 kg CO₂ kWh⁻¹) or gas (0.46 kg CO₂ kWh⁻¹)⁵⁸ that is substituted by PV and wind power, γ_x is the flux of the terrestrial carbon sink disaggregated from a bottom-up estimate⁵⁹ and ν_x is the concentration of soil carbon in lands covered by vegetation⁶⁰ transferred to PV panels or wind turbines (Supplementary Table 9).

We derived the MAC for a new PV or wind power plant ϵ , MAC_ϵ , based on the abated CO₂ emissions:

$$\text{MAC}_\epsilon = \frac{\text{LCOE}_\epsilon \cdot E_\epsilon - \text{LCOE}_{\epsilon-1} \cdot E_{\epsilon-1} - \varrho \cdot (E_\epsilon - E_{\epsilon-1})}{F_\epsilon - F_{\epsilon-1}} \quad (10)$$

in which ϱ is the price of coal, oil or gas. We obtained the prices of coal (\$0.043 ± 0.015 per kWh as the 95% confidence interval)⁶¹, oil (\$0.141 ± 0.057 per kWh)^{62,63} and gas (\$0.058 ± 0.016 per kWh)⁶⁴ in China as the averages during 2010–2020, when they are considered

to generate electricity with an efficiency of 35%, 38% and 45%, respectively⁶⁵. The generation of power by fossil fuel in the 2010s in China was dominated by coal, with a contribution⁶⁶ of 96% in 2020, but the composition of fossil fuel in the future is as yet unknown for China. We assumed that the future fossil-fuel composition in China will be constant in our central case, but we performed two sensitivity experiments to consider the impact of changes in fuel composition. First, the share of oil for generating power increases from the current level in 2020 (0.3%) to 50% in 2060 by substituting coal when the share of gas is identical to that in the central case. Second, the share of gas for generating power increases from the current level in 2020 (4.1%) to 50% in 2060 by substituting coal when the share of oil is identical to that in the central case (Extended Data Fig. 6).

Hourly power demand

We predicted the hourly power demand by 2060 based on the flexibility of power loads by sector (Supplementary Table 10). First, we scaled up the historical hourly power loads from electrical grids⁶⁷ in 2018 by the increase in total power demand under the projected rate of electrification³³ in 2060 (58%) for six non-power sectors, including agriculture, industry, transport, building, service and household electric appliances, in 31 provinces. We assumed that the power loads are flexible for agriculture, industry, building, service and household electric appliances, except for heating and cooling in houses and electric cars, so we could simulate the profiles of the hourly power demand to match the hourly power generation by PV and wind endogenously in our optimization model. Second, we predicted the hourly power demand by electric cars. We obtained the profile of traffic flow in each street every five minutes in 2018 in Shenzhen⁶⁸, which was assumed to represent the variation of traffic flow in the future owing to a lack of data for other cities in China. When electricity is used by electric cars, one-third of vehicles are charged immediately, one-third are charged in one hour and one-third are charged in two hours²⁵.

Third, we predicted the hourly power loads for heating and cooling in houses. We obtained the hourly energy used for space heating and cooling in houses by region in China⁶⁹. Finally, we considered the impact of temperature on the power demand for heating and cooling in houses and electric cars based on the projected temperature under climate warming. The electricity used for heating increases by 0.98% as the annual average temperature decreases by 1 °C when the hourly temperature is below 16 °C (ref. 70), whereas the electricity used for cooling increases by 0.63% as the annual average temperature increases by 1 °C when the hourly temperature is above 28 °C (ref. 25). We predicted the hourly power demand for heating and cooling for 31 provinces for 2021–2060 based on the gridded hourly temperature⁷¹ averaged for 2016–2020 and the projected change in annual average temperature during 2021–2060 under the SSP1-2.6 scenario from an Earth System Model¹⁷. The power demand shifts in the daytime to match the peak of hourly PV and wind power generation (Supplementary Fig. 5).

Actual PV and wind power plants

We adopted a pixel resolution of $1 \times 3 \text{ km}^2$ for installing PV panels or wind turbines, which allows us to predict the location and capacity of individual PV and wind power plants in our optimization model. We cannot validate the locations and capacities of the projected PV or wind power plants that had not yet been built, so we used the locations and capacities of the commissioned PV and wind power plants in OpenStreetMap³¹ that were closest to the projected PV or wind power plants to evaluate our prediction (Extended Data Fig. 3). We estimated the geographical distance of locations between the projected and actual PV and wind power plants. A full validation of our optimization model required detailed information on the PV and wind power plants when they are to be built in the coming decades, so we only compare the projected capacities of power plants normalized by current area with the actual capacities of the existing power plants in OpenStreetMap³¹.

Distribution of income

We estimated the impact of finances embodied in the flow of electricity generated by new PV and wind power plants on the redistribution of income in 2060. First, we estimated the distribution of income among the population at a county level based on the frequency distribution of income among the residents of urban and rural populations derived from a national survey⁷² in 2015. We considered that the annual growth rate of population is 2% for Gansu, Inner Mongolia, Ningxia, Qinghai, Xinjiang and Xizang, which is higher than other provinces (1%) resulting from more new jobs and higher income created in these less-developed provinces⁶⁶. Second, we compiled the per-capita disposable income for urban and rural populations at the county level⁶⁶ for 2015–2019. We made a linear projection of per-capita disposable income to 2060 based on the rate of growth of income by province during 2021–2060. We calibrated the growth rate of per-capita income for each income group at the county level during 2015–2060 to guarantee that the projected per-capita income as an average for each county in 2060 was equal to the projection for 2060. Given a carbon price (ζ), we assumed that only power plants with MACs below this carbon price were constructed. We estimated the revenue (R_ϵ) from power generation when building a new PV or wind power plant (ϵ):

$$R_\epsilon = \varrho \cdot E_\epsilon + \zeta \cdot F_\epsilon - \text{LCOE}_\epsilon \cdot E_\epsilon \quad (11)$$

in which ϱ is the price of coal, oil or gas in China that is substituted by PV or wind power, F_ϵ is total abatement of CO₂ emissions, E_ϵ is total PV and wind power generation and LCOE _{ϵ} is the LCOE for the projected PV and wind power plants after building plant ϵ .

Revenue from PV and wind power generation could be derived from the electricity price minus the LCOE, but the electricity price can be influenced by many socio-political factors^{25,50}. We focused on analysing the impact of carbon price as a proxy for climate policies on the revenue of PV and wind power, so we considered that the electricity price depends on the fossil fuel prices and carbon price. The prices of fossil fuel may increase in the future owing to the scarcity of fossil fuel⁷³, which can increase the revenue of replacing fossil fuel with renewables, including PV and wind power. To estimate the prices of fossil fuel in 2060, we randomly draw the prices from the normal distributions, the average and standard deviations of which are estimated from the prices that are available from 2010 to 2020 (Extended Data Fig. 6). Predicting the impact of energy scarcity on the prices of fossil fuel and thus the revenue of PV and wind power is not considered in this study.

We represented the income inequality by dividing the population into 2,002 groups based on the order of income in each county. We excluded pixels in urban areas for the construction of utility-scale PV or wind power plants, so we allocated the revenue among the rural population in each county. When a carbon tax was levied on fossil fuels, we predicted the change in the per-capita income for each group in the population by considering the increased costs of power generation, the revenue from PV and wind power generation and the costs of carbon tax saved by reducing the use of fossil fuel (Supplementary Method 9). Finally, we estimated the income Gini coefficient in China using a formula⁷⁴ based on the changes in the fractions of income and population in each population group for 2,373 counties in 2060 when the carbon price increases from \$0 to \$100 per tCO₂.

Uncertainty analyses

We estimated the uncertainties in the MAC and the Gini coefficient by running an ensemble of Monte Carlo simulations 40,000 times⁷⁵. We randomly varied the parameters in these simulations, including: (1) the variability of PV power generation ($\pm 5\%$) over a suitable pixel (W_{ijv}) owing to the impact of aerosol deposition on PV panels⁷⁶ and the variability of wind power generation ($\pm 2\%$) over a suitable pixel (W_{ijw}) owing to the

impact of climate change on wind resources⁷⁷, (2) the growth rate of power demand by province during 2020–2060 ($\pm 1\%$)⁷, (3) the parameters used in the calculation of initial investment costs based on the variability of capital costs ($\pm 10\%$) from previous estimates^{55,56}, (4) the historical rates of learning for different cost components measured in China (Supplementary Table 1) and (5) the parameters used for calculating the costs of UHV transmission and energy storage from different studies (Supplementary Table 8). Last, we adopted the medians of the MAC and the Gini coefficient to represent our best estimates, whereas we used the 90% uncertainties and interquartile ranges to represent their uncertainties.

Data availability

Data used in this study are publicly available at the Zenodo repository: <https://zenodo.org/record/7963012#.ZGzUd31Bw2w>. General Electric model and Vestas model in the Windturbines database: <https://en.wind-turbine-models.com/turbines>; MCD12Q1 dataset: <https://lpdaac.usgs.gov/products/mcd12q1v006/>; GEOS-5 dataset: https://opendap.nccs.nasa.gov/dods/GEOS-5/fp/0.25_deg/assim; Maritime Boundaries Geodatabase: <http://www.vliz.be/en/imis?dasid=5465&doiid=312>; Mask of terrestrial ecological reserve: <http://www.resdc.cn/data.aspx?DATAID=137>; marine ecological reserve: <https://www.protectedplanet.net/country/CHN>; Radar Topography Mission (SRTM) Global Enhanced Slope (GES) dataset: <https://lpdaac.usgs.gov/products/srtmg1v003/>; MERRA-2 dataset: https://disc.gsfc.nasa.gov/datasets/M2T1NXADG_5.12.4/summary?keywords=SO2.

Code availability

Further material is available in the Supplementary Information. The model used in this study can be accessed at the Zenodo repository: <https://zenodo.org/record/7963012#.ZGzUd31Bw2w>.

- United States Geological Survey (USGS). Land cover type yearly L3 global 500 m SIN grid <https://lpdaac.usgs.gov/products/mcd12q1v006/> (2014).
- Report for the Grid Parity of China's Wind Power (in Chinese) (CWEA, 2020); <https://finance.sina.com.cn/stock/stockzmt/2020-05-14/doc-irczymk1651936.shtml>.
- Bauer, L. & Matysik, S. Windturbines database. <https://en.wind-turbine-models.com/turbines> (2021).
- Cole, W. J. & Frazier, A. W. Cost projections for utility-scale battery storage. Report number NREL/TP-6A20-73222. *National Renewable Energy Laboratory* <https://www.nrel.gov/docs/fy19osti/73222.pdf> (2019).
- Yan, J., Yang, Y., Campana, P. E. & He, J. City-level analysis of subsidy-free solar photovoltaic electricity price, profits and grid parity in China. *Nat. Energy* **4**, 709–717 (2019).
- Xiang, C., Chen, F., Wen, F. & Song, F. Can China's offshore wind power achieve grid parity in time? *Int. J. Green Energy* **18**, 1219–1228 (2021).
- Popp, D. Induced innovation and energy prices. *Am. Econ. Rev.* **92**, 160–180 (2002).
- Electric Power Planning and Engineering Institute. *Power Grid Engineering Quota Design Control Index* (China Electric Power Press, 2020); <https://www.doc88.com/p-93447011586773.html>.
- China Renewable Energy Engineering Institute. *Construction Land Index of Power Engineering Project (Wind Farm)* (China Electric Power Press, 2012).
- China PV industry development roadmap. *CPIA* http://www.chinapv.org.cn/road_map/927.html (2021).
- Liu, Z., Zhang, W., Zhao, C. & Yuan, J. The economics of wind power in China and policy implications. *Energies* **8**, 1529–1546 (2015).
- Sherman, P., Chen, X. & McElroy, M. B. Offshore wind: an opportunity for cost-competitive decarbonization of China's energy economy. *Sci. Adv.* **6**, eaax9571 (2020).
- Liu, Z. et al. Reduced carbon emission estimates from fossil fuel combustion and cement production in China. *Nature* **524**, 335–338 (2015).

- Jiang, F. et al. A comprehensive estimate of recent carbon sinks in China using both top-down and bottom-up approaches. *Sci. Rep.* **6**, 22130 (2016).
- Lai, L. et al. Carbon emissions from land-use change and management in China between 1990 and 2010. *Sci. Adv.* **2**, e1601063 (2016).
- China Qinhuangdao coal spot price from 2003 to 2019. *Statista* <https://www.statista.com/statistics/383534/asian-coal-marker-price/> (2021).
- Yte1. Fuel oil (180CST) price trend chart in 2022 <http://www.yte1.com/datas/ranliayouou-pri?end=2022> (2022).
- Domestic Fuel Oil Market Annual Analysis Report in 2011* (CNPC, 2012) <https://view.officeapps.live.com/op/view.aspx?src=http%3A%2F%2Foilinfo.cnpc.com.cn%2Fypxx%2Fyjnb%2F201208%2F24404fbc0eed4f2280939eae3c4ea8ad%2Ffiles%2F8920787449ee417997c0147be45fce98.doc&wdOrigin=BROWSELINK>.
- National Development and Reform Commission (NDRC). Price list of benchmark gate stations for non-residential natural gas in each province http://www.gov.cn/xinwen/2019-03/29/content_5378081.htm (2019).
- Zeiss, G. Energy efficiency of fossil fuel power generation <https://geospatial.blogs.com/geospatial/2010/01/energy-efficiency-of-fossil-fuel-power-generation.html> (2010).
- National Bureau of Statistics of China. *China Energy Statistical Yearbook 2020* (China Statistics Press, 2020).
- National Development and Reform Commission (NDRC). Typical power load curves of provincial power networks in China <https://www.gov.cn/zhengce/zhengceku/2020-12/03/5566580/files/ea9a93782e514543861bdcd434e86666.pdf> (2019).
- Shenzhen Municipal Government Data Open Platform. Street real-time data https://opendata.sz.gov.cn/data/dataSet/toDataDetails/29200_00403589 (2018).
- Zheng, X. & Wei, C. *Household Energy Consumption in China: 2016 Report* (Springer, 2019).
- General Administration of Quality Supervision, Inspection and Quarantine (GAQSIQ). Indoor air quality standard. GB/T 18883–2002. <https://www.mee.gov.cn/image20010518/5295.pdf> (2002).
- Global modelling and assimilation office. GEOS atmospheric assimilation products https://gmao.gsfc.nasa.gov/GMAO_products/NRT_products.php (2021).
- Zhang, T., Emanuel, A. E. & Orr, J. A. in *Proc. 2016 IEEE Power and Energy Society General Meeting (PESGM)* 1–5 (IEEE, 2016).
- Adelman, M. A. Scarcity and world oil prices. *Rev. Econ. Stat.* **68**, 387–397 (1986).
- Mi, Z. et al. Economic development and converging household carbon footprints in China. *Nat. Sustain.* **3**, 529–537 (2020).
- Sokal, R. R. & Rohlf, F. J. *Biometry: The Principles and Practice of Statistics in Biological Research* (W. H. Freeman, 1981).
- Li, X., Mauzerall, D. L. & Bergin, M. H. Global reduction of solar power generation efficiency due to aerosols and panel soiling. *Nat. Sustain.* **3**, 720–727 (2020).
- Gao, Y., Ma, S. & Wang, T. The impact of climate change on wind power abundance and variability in China. *Energy* **189**, 116215 (2019).

Acknowledgements We thank M. Harder for useful discussion. This study was funded by the National Key R&D Program of China (no. 2022YFF0802504), the National Natural Science Foundation of China (nos. 42341205 and 41877506) and the Chinese Young Thousand Talents programme. R.W., J. Chen, X.T. and R.Z. acknowledge support from the Shanghai International Science and Technology Partnership Project (no. 21230780200). K.T. benefited from state assistance managed by the National Research Agency in France under the Programme d'Investissements d'Avenir under the reference ANR-19-MPGA-0008. P.C. acknowledges support from the ANR CLAND Convergence Institute 16-CONV-0003. J.P. and J.S. acknowledge the financial support from the Catalan Government grant SGR 2021-1333, the Spanish Government grants PID2019-110521GB-I00, PID2020-115770RB-I00 and TED2021-132627B-I00 funded by MCIN, AEI/10.13039/501100011033 funded by the European Union Next Generation EU/PRTR and the Fundación Ramón Areces grant C1VP20A6621.

Author contributions R.W. initiated the study, led the project and designed the research. Y.W. compiled data, performed the research and prepared graphs. W.L., X.X., J.L., S.X., Y.X. and R.Y. provided analysing tools. K.T. contributed to economic analysis. P.C., K.T., J.P., Y.B., J.S. and D.H. contributed to energy analysis. K.T., J. Cao, J. Chen, L.W., X.T. and R.Z. contributed to policy analysis. R.W. wrote the first draft of the paper. All authors critically revised successive drafts of the paper and approved the final version.

Competing interests The authors declare no competing interests.

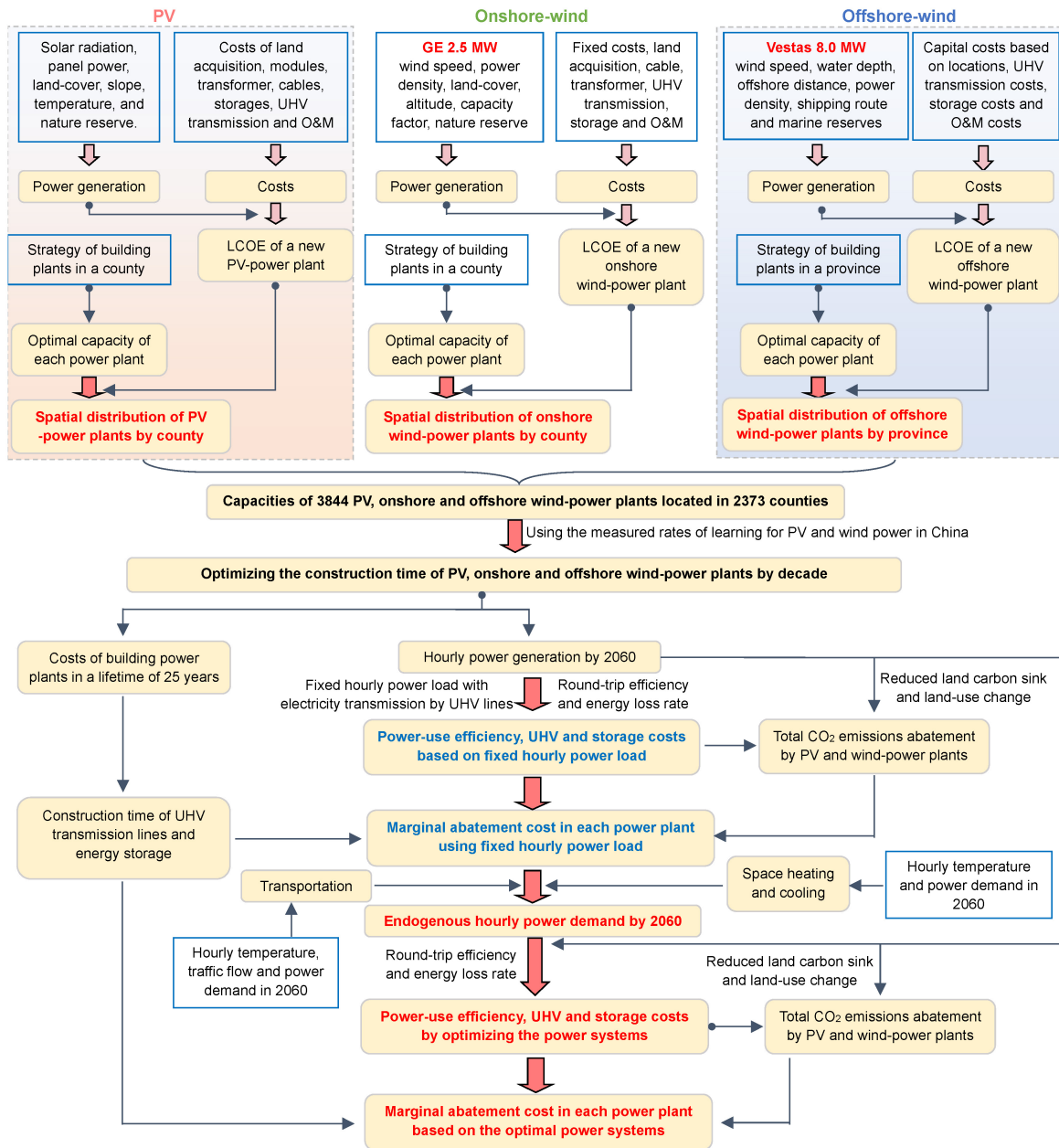
Additional information

Supplementary information The online version contains supplementary material available at <https://doi.org/10.1038/s41586-023-06180-8>.

Correspondence and requests for materials should be addressed to Rong Wang.

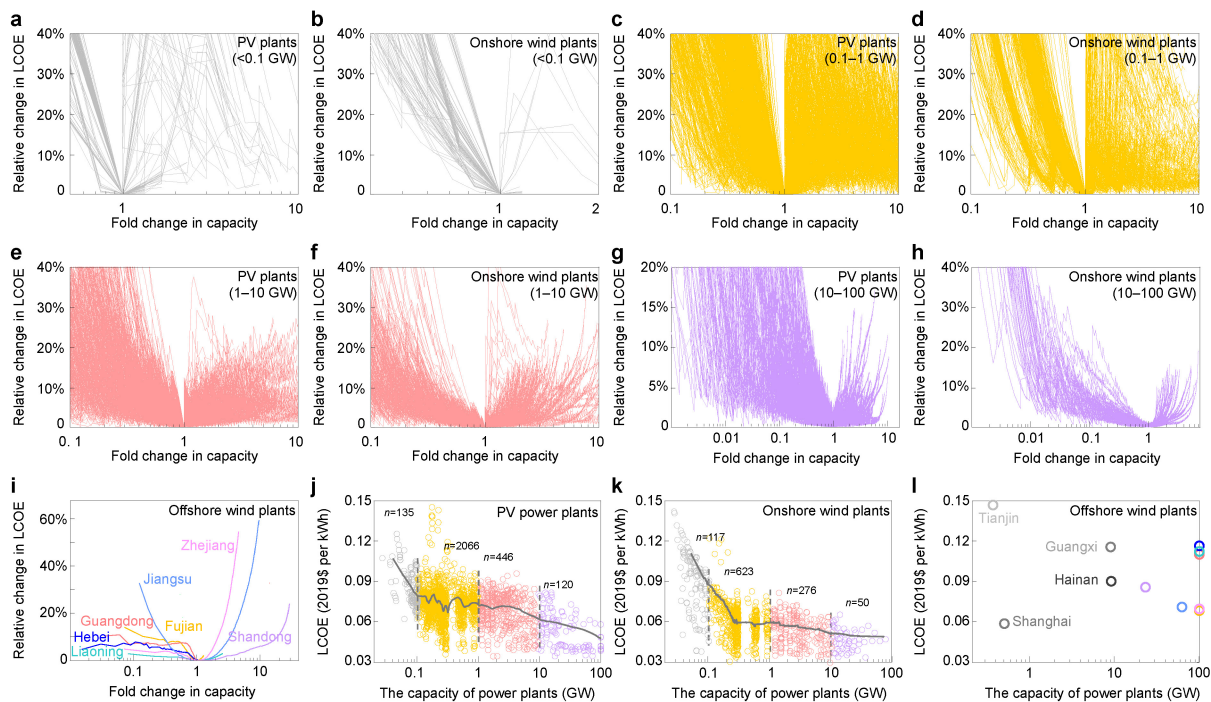
Peer review information *Nature* thanks Aleh Cherp, Gang He and the other, anonymous, reviewer(s) for their contribution to the peer review of this work. Peer reviewer reports are available.

Reprints and permissions information is available at <http://www.nature.com/reprints>.



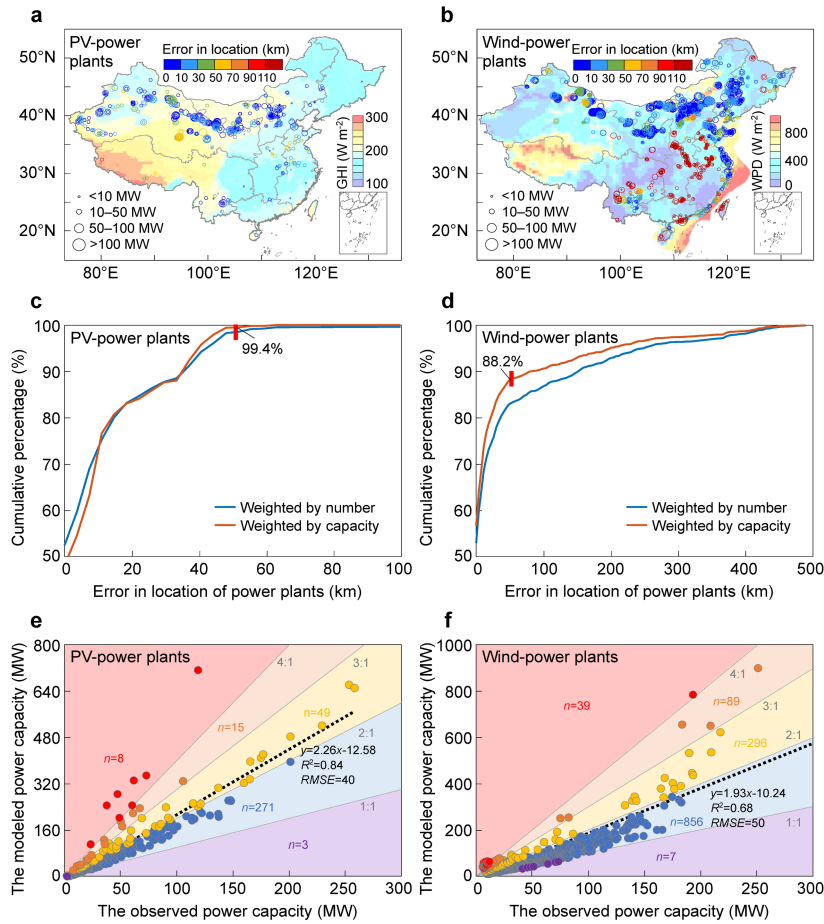
Extended Data Fig. 1 | Procedures for optimizing the location, capacity and construction time of new PV and wind power plants in China. The LCOE indicates the grid parity of PV and wind power generation coordinated with electricity transmission and energy storage in the power systems. We take the

number of pixels installing PV panels or wind turbines and the construction time of each PV or wind power plant by decade as the decision variables to minimize the LCOE of all PV and wind power plants.



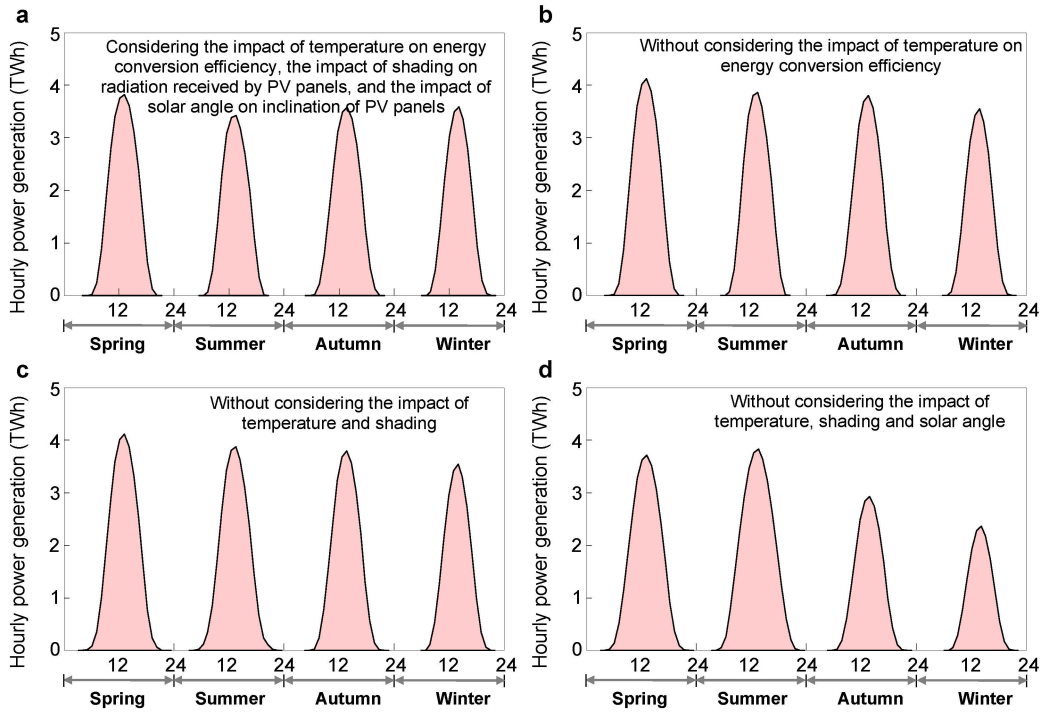
Extended Data Fig. 2 | Impact of increasing the power capacity of PV or wind power plants on the LCOE. **a–h**, Relative change in the LCOE as a percentage relative to the minimum when increasing the capacity of each PV (**a,c,e,g**) or onshore wind (**b,d,f,h**) power plant. The power plants are categorized into four groups, the optimized capacity of which falls in the range <0.1 GW (**a,b**), 0.1–1 GW (**c,d**), 1–10 GW (**e,f**) and 10–100 GW (**g,h**). **i**, Relative change in the LCOE as a percentage relative to the minimum when increasing the capacity of each offshore wind power plant. We estimate the fold change in the capacity

of each power plant when increasing the number of pixels installing PV panels or wind turbines relative to the optimal capacity reaching the minimum of the LCOE for each power plant. **j–l**, Relationship between the minimum of the LCOE and the optimal capacity (<100 GW) of the projected PV (**j**), onshore wind (**k**) and offshore wind (**l**) power plants. The power plants are categorized into four groups based on the optimal capacity, for which the moving averages for 50 plants are shown by the grey lines in **j** and **k**.



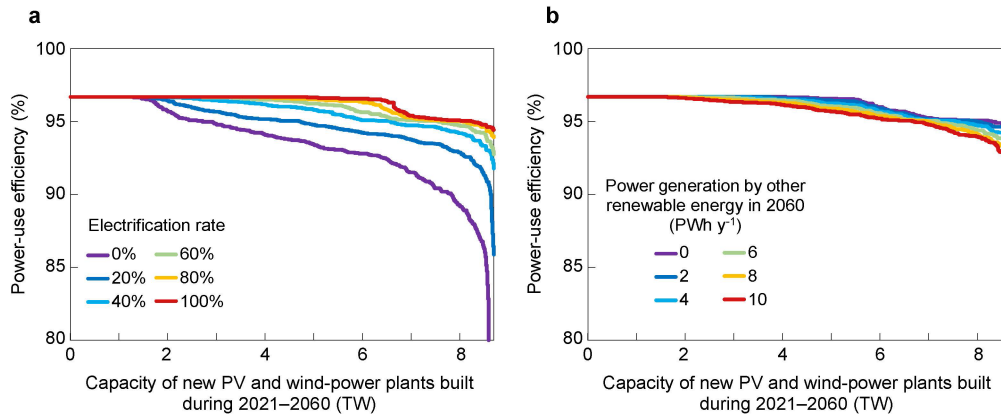
Extended Data Fig. 3 | Evaluation of the location and capacity of PV and wind power plants in our optimization model. a, b, Difference in the predicted location of PV (a) and wind (b) power plants in our optimization model relative to the location of PV panels and wind turbines installation observed by OpenStreetMap³¹. **c, d,** Frequency distribution of the difference

in the location of PV (c) and wind (d) power plants weighted by the number of power plants (blue line) or the capacity of power plants (red line). **e, f,** Comparison of the projected capacity of PV (e) and wind (f) power plants in our optimization model normalized by the area of power plants with the capacity of PV and wind power plants observed by OpenStreetMap³¹.



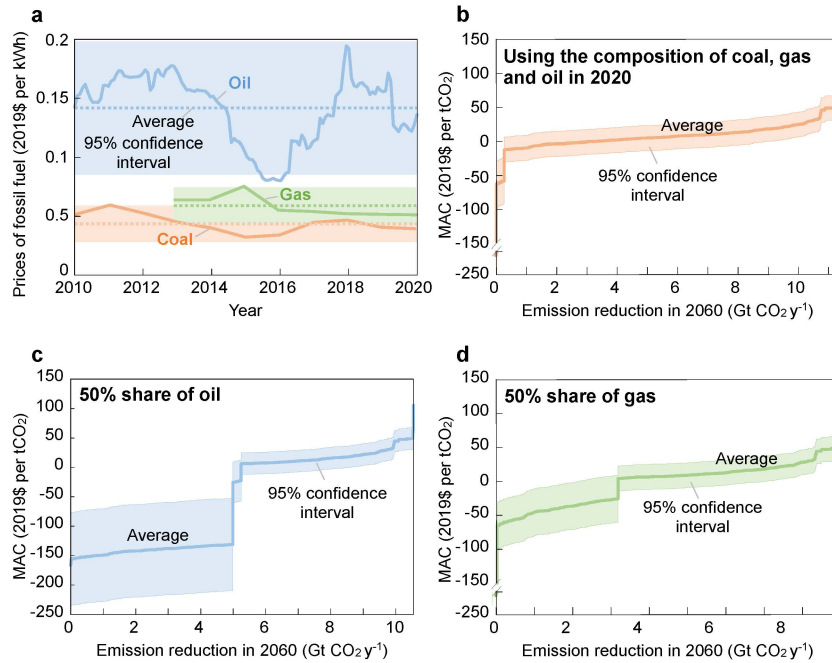
Extended Data Fig. 4 | Seasonal variations in the hourly power generation by PV plants. **a**, Hourly power generation by PV plants by considering the impact of temperature on energy-conversion efficiency, the impact of shading on radiation received by PV panels and the impact of solar angle on the inclination

of PV panels. **b–d**, Hourly power generation by PV plants in sensitivity tests without considering the impact of temperature on energy-conversion efficiency (**b**), without considering the impact of temperature and shading (**c**) or without considering the impact of temperature, shading and solar angle (**d**).



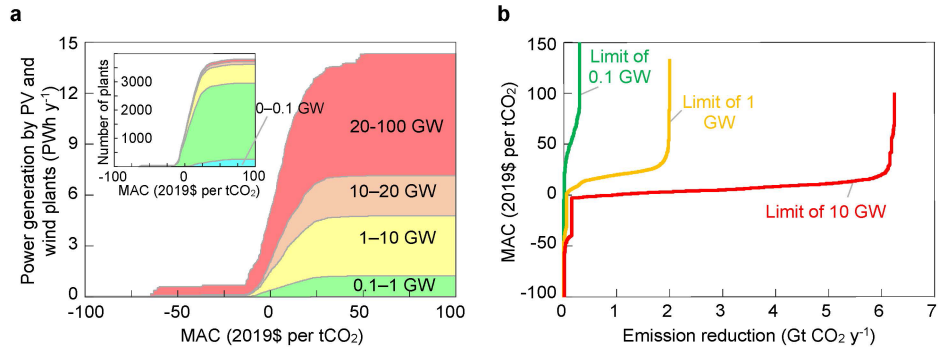
Extended Data Fig. 5 | Impact of the rate of electrification and the power generation by other renewables in 2060 on the power-use efficiency for PV and wind power plants in China. By considering the flexible power load with UHV and energy storage, the power-use efficiency for PV and wind power plants

is estimated when the electrification rate in 2060 increases from 0 to 20%, 40%, 60%, 80% and 100% (a) and the power generation by other renewables in 2060 increases from 0 to 2, 4, 6, 8 and 10 PWh year⁻¹ (b).



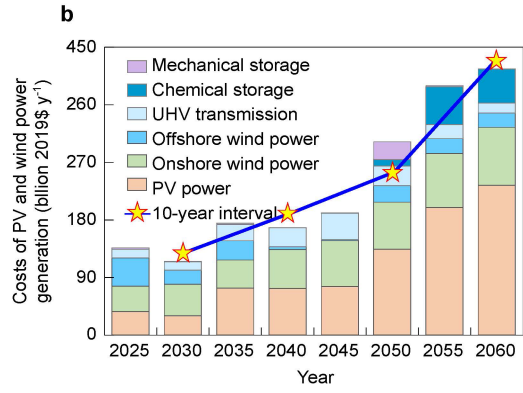
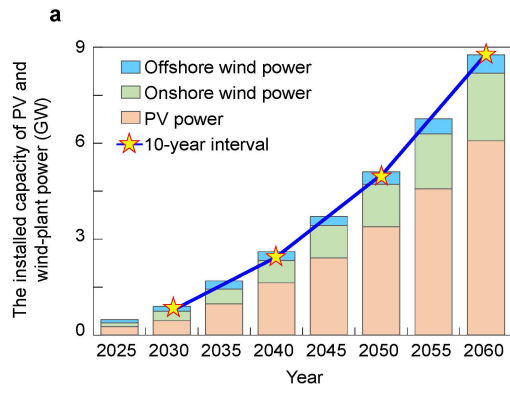
Extended Data Fig. 6 | Impact of the fossil fuel composition on the MAC for PV and wind power plants in 2060. **a**, Prices of coal, oil and gas for power generation in China during 2010–2020. The solid line denotes the average price, whereas the shading denotes the 95% confidence interval. **b**, MAC for PV and wind power plants in the central case, in which the consumption of coal, oil and gas for 2021–2060 are projected by scaling up the consumption in 2020 with the projected growth of total power demand. **c**, As in **b** but for a sensitivity

case in which the share of oil in electricity generation increases linearly from the current level in 2020 (0.3%) to 50% in 2060 by replacing coal, but the share of gas is identical to the central case. **d**, As in **b** but for a sensitivity case in which the share of gas in electricity generation increases linearly from the current level in 2020 (4.1%) to 50% in 2060 by replacing coal, but the share of oil is identical to the central case.



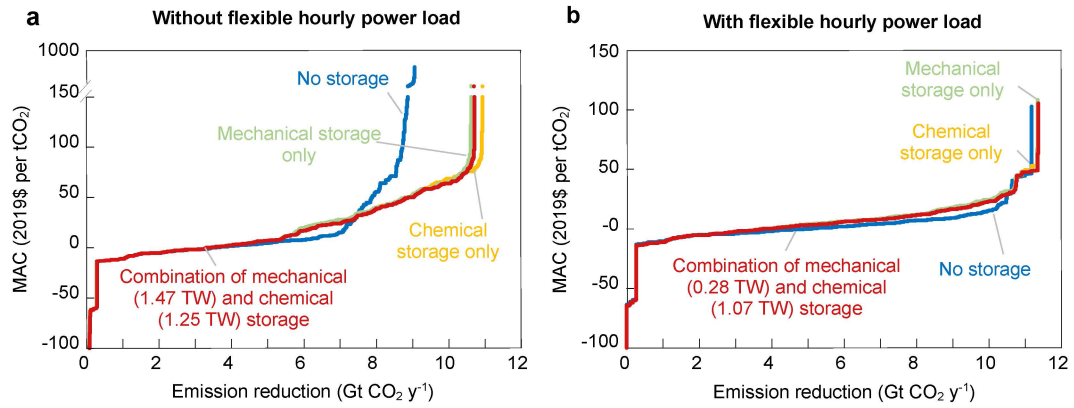
Extended Data Fig. 7 | Impact of changing the limit of the capacity of PV and wind power plants on the MAC in 2060. a, Composition of power generation by PV and wind plants. The inset shows the number of PV and wind power plants.

b, The MAC for PV and wind power when the capacity of individual power plants is limited to 0.1 GW (green), 1 GW (orange) and 10 GW (red), respectively.



Extended Data Fig. 8 | Impact of changing the interval of optimization on the installed capacity and costs of PV and wind power plants built during 2020–2060. The installed capacity (a) and costs (b) of PV and wind power

plants built during 2020–2060 are estimated in our model by optimizing the construction time of individual power plants at a temporal interval of 5 years (bars) or 10 years (stars).



Extended Data Fig. 9 | Impact of adopting different strategies of energy storage on the MAC of PV and wind power in China. MACs of PV and wind power in 2060 are estimated in the scenarios without (a) or with (b) considering the flexible hourly power load. We compare MACs in the sensitivity tests without storing energy (blue line), using mechanical storage (pumped hydro) for all

power plants (green line), using chemical storage (batteries) for all power plants (orange line) or using the optimized strategy of energy storage for each power plant in the central case (red line). We show the total capacity of mechanical (pumped hydro) and chemical (batteries) storage in the central case.

Extended Data Table 1 | Distribution of pixels installing PV panels or wind turbines

Land-cover	Area (km ²)			
	PV	Onshore-wind	Offshore-wind	Total
Closed Shrubland	22 (0%)	76 (0.01%)	0 (0%)	97 (0.01%)
Open Shrubland	247 (0.04%)	101 (0.02%)	0 (0%)	348 (0.03%)
Woody savanna	26487 (4.5%)	7323 (1.34%)	0 (0%)	33213 (3%)
Savanna	44857 (7.7%)	15759 (2.88%)	0 (0%)	59280 (5.3%)
Grassland	226923 (39%)	265175 (48%)	0 (0%)	392156 (35%)
Croplands	0 (0%)	70562 (13%)	0 (0%)	70562 (6%)
Vegetation mosaics	0 (0%)	4009 (0.73%)	0 (0%)	4009 (0.36%)
Snow, ice	1137 (0.19%)	0 (0%)	0 (0%)	1137 (0.1%)
Desert	284989 (48%)	184324 (34%)	0 (0%)	375351 (33%)
Water bodies	0 (0%)	0 (0%)	188485 (100%)	188485 (16%)
Total	584661 (100%)	547329 (100%)	188485 (100%)	1124637 (100%)